Microstructural change near the martensitic transformation in a ferromagnetic shape memory alloy Ni51Fe22Ga27 studied by electron holography

Microstructural change near the martensitic transformation in a ferromagnetic shape memory alloy Ni$_{51}$Fe$_{22}$Ga$_{27}$ studied by electron holography

Y. Murakami[a)] and D. Shindo
Institute of Multidisciplinary Research for Advanced Materials, Tohoku University, Sendai 980-8577, Japan

K. Oikawa
National Institute of Advanced Industrial Science and Technology, Tohoku Center, Sendai 983-8551, Japan

R. Kainuma and K. Ishida
Department of Metallurgy, Graduate School of Engineering, Tohoku University, Sendai 980-8579, Japan

Temperature dependence of the magnetic microstructure in a ferromagnetic shape memory alloy Ni$_{51}$Fe$_{22}$Ga$_{27}$ has been studied by electron holography, by which the distribution of magnetic flux is clearly imaged. Although the magnetic flux is quite even in the parent phase near room temperature, it undergoes considerable modulation when the temperature approaches M_s (martensitic transformation start temperature). The magnetization distribution in the martensite appears to be inherited from that in the parent phase. The observations shed further light on the precursor phenomenon of martensitic transformations. © 2004 American Institute of Physics.
[DOI: 10.1063/1.1841471]

Detailed observations of magnetic domains are vital when exploring huge deformation in ferromagnetic shape memory alloys (SMAs).[1–4] These deformations, which originate from a rearrangement of martensite variants (twins) in an applied magnetic field, have attracted the attention of researchers in the past decade because of their potential application in actuators. In fact the magnetic domains of martensites have been observed by a variety of techniques such as magnetic force microscopy,[5] a colloidal method,[6] Lorentz microscopy,[7] electron holography,[8] etc. Several studies claim that correspondence between the magnetic domains and the martensite variants (crystallographic domains) is essential, i.e., the magnetization vector of each martensite variant is in principle parallel to the easy magnetization axis. The observations may prove to be a key to support a theory that stresses the impact of the magnetocrystalline anisotropy of martensites on the achievement of detwinning in an applied magnetic field.[1,9,10]

In contrast, the magnetic anisotropy in the cubic parent phase is approximately two orders of magnitude lower than that of martensites with a lower crystallographic symmetry (tetragonal, orthorhombic, monoclinic, etc.). As a consequence of the low magnetic anisotropy, the magnetic domain structure of the parent phase is much more sensitive to crystallographic defects and/or distortions. Owing to this magnetoelastic coupling, we can expect the magnetic domains to provide essential information regarding the lattice modulation in the parent phase, e.g., feature of $\langle 110 \rangle \langle 1\bar{1}0 \rangle$-type transverse displacement waves that are widely observed in the parent phase of SMAs.[11–14] Note that a detailed observation of the faint lattice modulation is not easy with conventional diffraction techniques, while the magnetic domains may show an appreciable change as the lattice modulation develops by cooling. In fact recent Lorentz microscopy studies have reported desirable changes in the magnetic domains

near M_s (martensitic transformation start temperature).[8,15] The purpose of the present study is to examine the temperature dependence of magnetic domains in Ni$_{51}$Fe$_{22}$Ga$_{27}$,[16] which is a recently developed ferromagnetic SMA, and to compare the magnetic microstructures between the parent phase and martensite.

The Ni$_{51}$Fe$_{22}$Ga$_{27}$ alloys were heat treated at 1473 K for 24 h to obtain a homogeneous single phase followed by quenching in ice water. The parent phase is L2$_1$ ordered and it transforms to the monoclinic martensite (10M structure) near 141 K. The Curie temperature (T_C) was evaluated at 310 K, which was defined as the minimum point of the temperature derivative of magnetization in the thermomagnetization curve. The magnetic domains were observed by Lorentz microscopy (to obtain images of the magnetic domain walls) and electron holography (to image magnetic flux)[17] using a transmission electron microscope JEM-3000F, to which a special pole piece producing only a low magnetic field (0.2 mT) was attached. Energy-filtered electron diffraction patterns, in which the strong background due to inelastic scattering is removed, were obtained by a microscope JEM-2010Ω.[18]

Figure 1(a) shows the temperature dependence of the magnetization in a Ni$_{51}$Fe$_{22}$Ga$_{27}$ alloy in magnetic fields of 59 Oe, 1 kOe, and 15 kOe.[16] Near room temperature, the magnetization in the parent phase increases with cooling. However, the observable magnetization is depressed in the lower temperature range of the parent phase as shown in the curves of 1 kOe and 59 Oe. Due to this depression, the observable magnetization slightly increases when the specimen transforms to the martensite at the arrows—note that the observable magnetization is generally reduced at a transformation point due to the high magnetocrystalline anisotropy of the martensite. In contrast, the depression of magnetization in the parent phase is obscured when the thermomagnetization curve is measured in a higher magnetic field of 15 kOe.

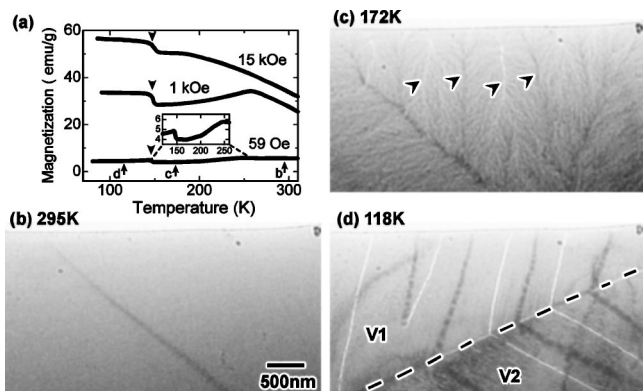a)Electronic mail: murakami@tagen.tohoku.ac.jp

FIG. 1. (a) Thermomagnetization curves of a $Ni_{51}Fe_{22}Ga_{27}$ alloy heat-treated at 1473 K. Although these curves were measured on warming, features of the temperature dependence are essentially the same as the curves measured on cooling. The inset shows an enlarged picture of the curve of 59 Oe. (b)–(d) Lorentz micrographs of the parent phase (295 and 172 K) and martensite (118 K). The broken line in (d) represents the interface of the martensite variants V1 and V2.

FIG. 2. Change in the reconstructed phase images with cooling in a $Ni_{51}Fe_{22}Ga_{27}$ alloy heat-treated at 1473 K. The images were obtained for the same area as those of Figs. 1(b)–1(d). Black lines represent the lines of magnetic flux projected along the incident electron beam. Arrows indicate the direction of magnetic flux.

The temperature dependence of the magnetic domains was examined by Lorentz microscopy as shown in Figs. 1(b)–1(d). Since the experiments were carried out using a magnetic-shielded objective lens, the Lorentz micrographs should be compared with the thermomagnetization curve measured in a low magnetic field (59 Oe or 1 kOe) rather than 15 kOe. At 295 K, the specimen shows large magnetic domains exceeding 1 μm—there is only one straight magnetic domain wall (dark line) in the field of view. However, the magnetic domain structure changes dramatically when the same region is observed at 172 K in the parent phase. Two types of changes are observed: (1) division of the original micrometer-scaled domain into ones on the order of 10^2 nm—see the new domain walls as marked by the arrowheads; (2) formation of speckles (on the order of 10 nm) indicating local fluctuation of the magnetization distribution. At 118 K, two martensite variants (V1 and V2) have been formed in the field of view [Fig. 1(d)]. Each martensite variant consists of several plate-like magnetic domains.

Figure 2 collects reconstructed phase images of the holograms observed for the same field of view as that in Fig. 1. Lines of magnetic flux (black lines) are smooth inside the large domains at 295 K although their directions (arrows) abruptly change at the magnetic domain wall. At 172 K, the lines of magnetic flux undergo two distinct modulations that are consistent with the Lorentz micrographs: (1) modulation of magnetic flux that subdivides the original micrometer-scaled domains into the order of 10^2 nm—traced by arrows in Fig. 2(b); (2) local fluctuation (of the order of 10 nm) that is responsible for the speckles in Lorentz micrographs—note that the line of magnetic flux is no longer smooth as shown by the circles in Fig. 2(b). These modulations disappear once the specimen transforms to the martensite. A noteworthy point is that the magnetization distribution near M_s [Fig. 2(b)] is similar to that of the martensite [Fig. 2(c)].

The local fluctuation of magnetic flux, which is responsible for the speckles in Lorentz micrographs, appears to be due to the interaction between magnetic domain walls and antiphase boundaries (APBs) in the $L2_1$-ordered parent phase. That is, the domain wall energy can be minimized at the position of APBs, near which the ferromagnetism is likely to be depressed. Unfortunately it is not easy to give a
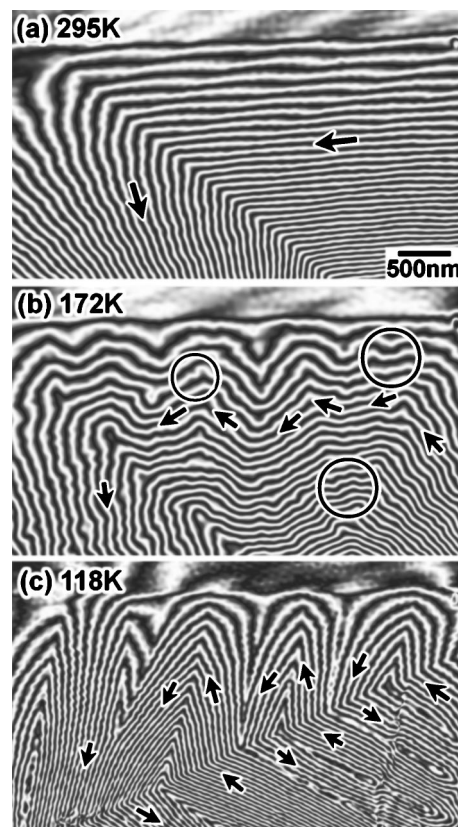
direct image showing one-to-one correspondence between APBs and magnetic domain walls since the size of the antiphase domains (APDs) is very small, i.e., 10–20 nm as shown in Fig. 3(a). Moreover, thermal drift in a lowered
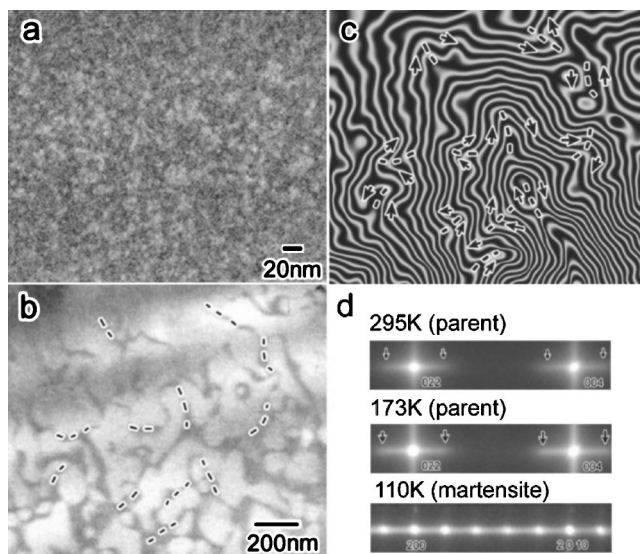

FIG. 3. Dark-field images obtained by using the 111-superlattice reflection in the parent phase of $Ni_{51}Fe_{22}Ga_{27}$ alloys heat-treated (a) at 1473 K and (b) at 1473 K followed by the subsequent heat-treatment at 773 K. (c) Reconstructed phase image in the parent phase at 199 K. The image was observed in the same area as that of (b). (d) Change in the electron diffraction patterns in a $Ni_{51}Fe_{22}Ga_{27}$ alloy heat-treated at 1473 K. Arrows in (d) represent the diffuse scattering in the parent phase.

temperature makes it difficult to take a hologram for the nanometer-scaled domains. Thus we have prepared another specimen with larger APDs [about 200 nm as shown Fig. 3(b)] by heat-treating a $Ni_{51}Fe_{22}Ga_{27}$ alloy at 773 K for 1 h followed by quenching in ice water. APBs are clearly imaged as dark regions and several APBs are traced by dotted lines. Note that the $L2_1$-ordered specimen in Fig. 3(b) also undergoes the subdivision of magnetic domains with cooling: the domain size is reduced to about 200 nm near M_s.[19] Figure 3(c) shows a reconstructed phase image at 199 K (above M_s by 17 K) observed in the same field of view as that of Fig. 3(b). It is clear that the lines of magnetic flux are bent at APBs—their directions (arrows) steeply change near the dotted lines, i.e., magnetic domain walls have been formed at APBs. The result explicitly indicates that the magnetic domain walls are stabilized at the positions of APBs. Development of the speckle contrast upon cooling as shown in Fig. 1(c) is regarded as a phenomenon related to demagnetization. Namely, the demagnetization energy can be substantially reduced by the formation of new magnetic domain walls at APBs (in the presence of many APBs), close to which magnetic charges appear due to the inhomogeneity of magnetization. The depression in the thermomagnetization curves of 1 kOe and 59 Oe [Fig. 1(a)] is also rationalized by the effect of APBs, i.e., with an increase in the population of the magnetic domain walls at APBs, a larger magnetic field is essential to achieve the fully magnetized state. However, in a higher magnetic field (15 kOe), the population of the domain walls should be substantially lower such that the depression in the thermomagnetization curve is obscured.

The other type of modulation, which subdivides the micrometer-scaled magnetic domains in the order of 10^2 nm as shown in Fig. 1(c), should be attributed to another source because of the distinct scale of length. A probable mechanism will be the lattice distortion due to the precursor phenomenon of martensitic transformations. As shown in Fig. 3(d), Bragg reflections of the parent phase are accompanied by rod-like diffuse scattering extending to 110-type directions in the reciprocal space. This diffuse scattering originates from $\langle 110 \rangle \langle 1\bar{1}0 \rangle$-type transverse displacement waves in the cubic parent phase. The lattice distortion appears to modify the magnetic microstructure in the parent phase via the magnetoelastic interaction. In fact the subdivision of the magnetic domains seems to be concurrent with the increase of the diffuse scattering intensity. More interestingly, the magnetization distribution near M_s [Fig. 2(b)] is quite similar to that in the martensite [Fig. 2(c)]—this is likely to be an indication that the subdivision of magnetic domains into the order of 10^2 nm is closely related to the precursor effect of the martensitic transformation.

A well-known microstructure related with the precursor effect of martensitic transformations is the tweed pattern,[11–14] i.e., striations along $\langle 110 \rangle$-type directions in the parent phase,

which originates from a static lattice displacement on {110} planes. In fact a bright-field image of $Ni_{51}Fe_{22}Ga_{27}$ showed a tweed contrast that was pronounced with cooling. The increase of the diffuse scattering intensity [Fig. 3(d)] is consistent with the development of the tweed contrast. The present study suggests that the tweed contrast may be spatially inhomogeneous, e.g., striations along [110] are especially strong in one region while those of [011] are dominant in the neighboring region, and these tweed patterns play an important role in the formation of specific martensite variants. Since the tweed contrast is sensitive to the diffraction condition too, more careful examinations are necessary to reach a conclusion. Nevertheless, the present observations of the magnetic microstructure, which is less sensitive to the diffraction condition, appear to be indicative of the inhomogeneous feature.

To summarize, this electron holography study has demonstrated a considerable interaction between APBs and magnetic domain walls in the parent phase of $Ni_{51}Fe_{22}Ga_{27}$. The present work also claims a similarity of magnetic microstructure between the parent phase near M_s and the martensite. The observations indicate that some elastic microstructure is produced by the $\langle 110 \rangle \langle 1\bar{1}0 \rangle$-type displacement waves in the parent phase and this microstructure plays an essential role in the formation of the martensite variants. The result is believed to be an essential feature of the precursor phenomenon of martensitic transformations.

[1]K. Ullakko, J. K. Huang, C. Kantner, R. C. O'Handley, and V. V. Kokorin, Appl. Phys. Lett. **69**, 1966 (1996).
[2]R. C. O'Handley, J. Appl. Phys. **83**, 326 (1998).
[3]M. Wuttig, J. Li, and C. Craciunescu, Scr. Mater. **44**, 2393 (2001).
[4]T. Kakeshita, T. Takeuchi, T. Fukuda, M. Tsujiguchi, T. Saburi, R. Oshima, and S. Muto, Appl. Phys. Lett. **77**, 1502 (2000).
[5]Q. Pan and R. D. James, J. Appl. Phys. **87**, 4702 (2000).
[6]H. D. Chopra, C. Ji, and V. V. Kokorin, Phys. Rev. B **61**, R14913 (2000).
[7]M. De Graef, M. A. Willard, M. E. McHenry, and Y. Zhu, IEEE Trans. Magn. **37**, 2663 (2001).
[8]Y. Murakami, D. Shindo, K. Oikawa, R. Kainuma, and K. Ishida, Acta Mater. **50**, 2173 (2001).
[9]R. D. James, and M. Wuttig, Philos. Mag. A **77**, 1273 (1998).
[10]T. Fukuda, T. Sakamoto, T. Kakeshita, T. Takeuchi, and K. Kishio, Mater. Trans., JIM **45**, 188 (2004).
[11]I. M. Robertson and C. M. Wauman, Philos. Mag. A **48**, 421 (1983).
[12]S. M. Shapiro, J. Z. Larse, Y. Noda, S. C. Moss, and L. E. Tanner, Phys. Rev. Lett. **57**, 3199 (1986).
[13]D. Schryvers and L. E. Tanner, Ultramicroscopy **32**, 241 (1990).
[14]Y. Murakami, H. Shibuya, and D. Shindo, J. Microsc. **203**, 22 (2001).
[15]A. Saxena, T. Castan, A Planes, M. Porta, Y Kishi, T. A. Lograsso, D. Viehland, M Wuttig, and M. De Graef, Phys. Rev. Lett. **92**, 197203 (2004).
[16]K. Oikawa, T. Ota, T. Ohmori, Y. Tanaka, H. Morito, A. Fujita, R. Kainuma, K. Fukamichi, and K. Ishida, Appl. Phys. Lett. **81**, 5201 (2002).
[17]D. Shindo and T. Oikawa, *Analytical Electron Microscopy for Materials Science* (Springer, Tokyo, 2002).
[18]Y. Murakami and D. Shindo, Mater. Trans., JIM **40**, 1092 (1999).
[19]Y. Murakami, D. Shindo, K. Oikawa, R. Kainuma, and K. Ishida, Appl. Phys. Lett. **82**, 3695 (2003).